

A Fast Adjustment Method of Magnetically Controlled Reactor with Multi-taps

Mengsen Liu^{1*}, Yongjian Li¹, Hezhe Gao¹, and Xuehai Gong²

¹State Key Laboratory of Reliability and Intelligence of Electrical Equipment, Hebei University of Technology, China

²Global Energy Interconnection Research Institute, China

(Received 15 July 2018, Received in final form 26 November 2018, Accepted 3 December 2018)

Magnetically controlled reactor (MCR) can compensate the capacitive reactive power generated by transmission line and enhance the stability of power supply, which is widely used in ultrahigh-voltage (UHV) power systems. In this paper, a novel structure for MCR with multi-taps is proposed. The MCR with multi-taps can switch its taps based on operation condition. The higher tap ratio is used to adjust the reactive power, and the lower tap ratio is fit for the stable grid. A switching algorithm is designed to make it work harmoniously and flexibly. For the adjustment of reactive power, this novel structure can perform better in regulated time without using higher tap ratios in practical operation, compared with the traditional structures.

Keywords : reactive power compensation, magnetically controlled reactor (MCR), fast adjustment method

1. Introduction

Magnetically controlled reactor (MCR) could effectively improve the stabilization of the electricity transmission system, increase the power factors, and restrain the over voltage of the system [1-3]. Due to the durable, efficient and affordable features, MCR has been favorably accepted by the grid, especially for ultrahigh-voltage (UHV) power systems [4, 5].

The reactance of an MCR can be changed by controlling the DC current through the control winding without adding DC exciting source, and the iron core of MCR can be saturated by adjusting the firing angle of thyristors [6]. The schematic diagram of the MCR with multi-taps is shown in Fig. 1. The MCR has two magnetic valves whose cross-sectional areas are smaller than that of the iron core. The design of magnetic valve will affect the current harmonics and capacity. Compared with the traditional design, the proposed MCR has two sets of power electronic switches with different tapping ratios denoted by the dotted box as shown in Fig. 1. The pro-

posed MCR has two tapping ratios, and therefore exhibits better control performance. In recent years, two stage MCRs have been implemented and reported to reduce the current harmonics [7, 8]. The other tough problem for the application of MCRs is its longer regulated time of reactive power [9]. As mentioned above, the variation of MCR reactance is controlled by changing the saturation of the magnetic valves, i.e., the regulated time of reactive power depends on the regulated time of DC current.

The tapping ratio of the MCR determines the regulated time, namely, higher tapping ratio could result in shorter regulated time, which is described by

$$n = \frac{1 - \delta}{2\delta} \quad (1)$$

where n and $\delta = N_1/N$ are the number of cycles and tapping ratio, respectively. The saturation degree of MCR should be 2π when the firing angle of the thyristors is zero theoretically. When the saturation degree of MCR is 2π , the MCR is fully saturated and the capacity of MCR reaches the maximum. If the design of magnetic valve cannot reach this point, most of the iron core material of MCR is wasted. Thus, δ should satisfy the following equation:

$$\delta = \frac{R^*}{1 - R^*} \quad (2)$$

©The Korean Magnetism Society. All rights reserved.

*Corresponding author: Tel: +86-13612197970

Fax: +86-13612197970, e-mail: 962294940@qq.com

This paper was presented at the IcaUMS2018, Jeju, Korea, June 3-7, 2018.

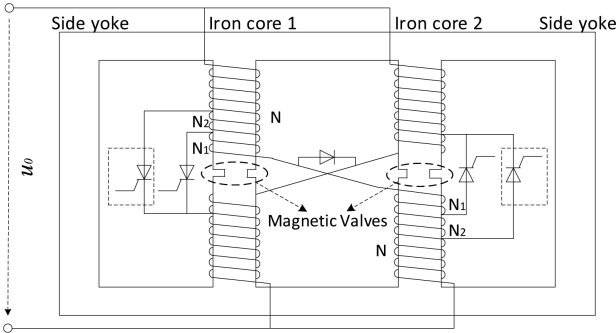


Fig. 1. Magnetically controlled reactor with multi-taps.

where $R^* = \frac{R}{2N\mu_0 U_0 / \pi B_{sat} l}$, R is the resistance of the

coil, l is the length of magnetic circuit, U_0 is the rated voltage, B_{sat} is the magnetic flux density when the iron core begins to saturate. If δ is higher than the value in (2), it will directly affect the economic operation of the MCR. Moreover, higher δ means higher copper loss, less stability, and larger current harmonics. There exists a contradiction between the performance optimization and economic operation of MCR. Usually, δ is set to less than 10 %.

Lower tapping ratio is applicable for small adjustment range while higher tapping ratio can provide better response in large adjustment range. Therefore, in this paper, a novel MCR containing two different tapping ratios is proposed to implement automatic switching under different working conditions. Meanwhile, an algorithm is built to switch taps smoothly.

2. Operating Principle of MCR with Multi-Taps

The principle of MCR is different from that of static var generator (SVG), which takes advantage of the nonlinearity of magnetic materials. SVG uses power switching tube to generate adjustable inductive current, while MCR generates adjustable inductive current by saturating iron cores [10]. The MCR has symmetrical structures, and it can be placed in the middle. One works in the positive half-cycle of AC current, and the other works in the negative half-cycle. When the current flows through one of them, the other is not working. Because the magnetic valve of that one is not saturated, and there is little current flowing in that branch.

The analysis of MCR is based on the two assumptions:

- (1) The magnetic flux density is uniform in the core.
- (2) Edge effect and leakage flux are small and therefore neglected.

When A_{s0} approaches to saturate, the following equation

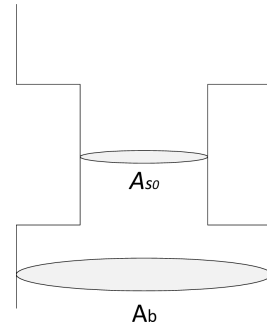


Fig. 2. Simplified magnetic valve of MCR.

can be obtained:

$$\Phi = BA_b = \mu_0 f(B)(A_b - A_{s0}) + BA_{s0} \quad (3)$$

where B is the magnetic flux density in the iron core.

Define the saturated magnetic flux density of the iron core as B_{sat} . The expression of equivalent $B-H$ characteristics for the magnetic valves, H as a function of B , can be written as

$$H(B) = \begin{cases} 0, & |B| < B_{sat} \\ \frac{B - B_{sat}}{\mu_0}, & B \geq B_{sat} \\ \frac{B + B_{sat}}{\mu_0}, & B \leq -B_{sat} \end{cases} \quad (4)$$

According to the structure of MCR with multi-taps as shown in Figs. 1 and 2, the corresponding equivalent circuit and $B-H$ curve of the magnetic valve are shown in Figs. 3 and 4. Because of the switching conditions of the thyristors and diodes, there exists a direct current flowing in the windings. It is worth noting that the two windings of the same iron core are not series connected. MCR has two independent direct current circuits, and they can be controlled by regulating the triggering angles of the

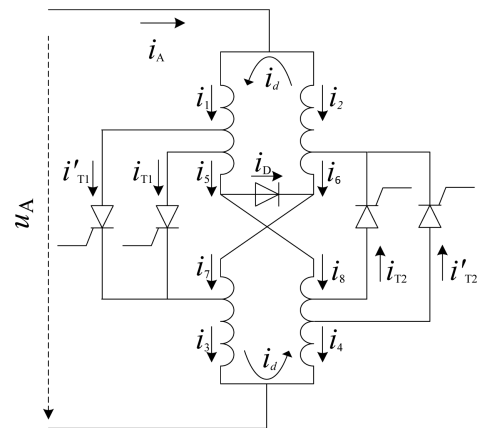


Fig. 3. Equivalent circuit of MCR with multi-taps.

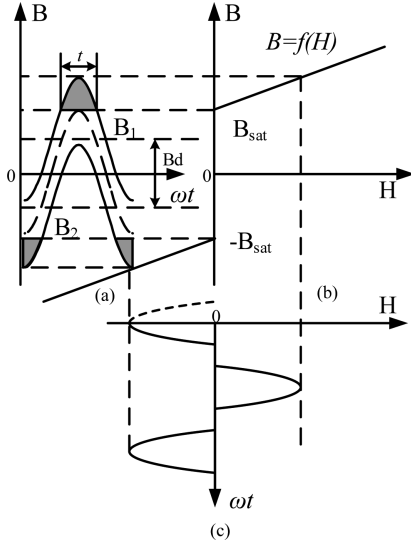


Fig. 4. Operating principle of MCR: (a) B of iron cores 1 and 2 varying with time, (b) Equivalent B - H characteristics of the magnetic valves in the iron cores, and (c) H of MCR varying with time.

thyristors. The free-wheeling diode provides constant current to ensure biased magnetic field to remain constant. According to the nonlinear curve shown in Fig. 4(b), when the thyristors are not triggered, magnetic field intensity of MCR is zero during a period. It means that the output current of MCR is zero, as indicated in Fig. 4(a) by the dashed lines. However, when the biased magnetic field is established, the magnetic flux densities of iron core 1 and iron core 2 are given by the solid lines in Fig. 4(a). From Fig. 4(a), when $B_1 > B_{sat}$ or $B_2 < -B_{sat}$, the magnetic valves are saturated and the magnetic field intensities of the magnetic valves vary with B . t is the period of time when H is not zero, and also represents the saturation degree of the magnetic valves.

As shown in Figs. 1 and 3, the structures of reactor and windings are symmetrical, so the following equations can be obtained.

$$i_d = I_0 + \sum_{k=2n}^{\infty} I_{km} \sin(k\omega t + \psi_k)$$

$$\frac{1}{2}i_A = \sum_{k=2n-1}^{\infty} I_{km} \sin(k\omega t + \psi_k)$$
(5)

Eq. (5) can be expressed in another way by using Fourier decomposition:

$$i_1 = \frac{1}{2}i_A + i_d$$

$$i_2 = \frac{1}{2}i_A - i_d$$
(6)

where i_1 and i_2 are the AC components of the two windings as shown in Fig. 3. To simplify the status of MCR equation, a state variable m is defined:

$$m = \begin{cases} 0, & 0 \leq \omega t < \alpha \\ 1, & \alpha \leq \omega t < \pi \\ 0, & \pi \leq \omega t < \pi + \alpha \\ -1, & \pi + \alpha \leq \omega t < 2\pi \end{cases} \quad (7)$$

where α is the firing angle of the thyristors. The current of MCR during a cycle can be expressed as

$$\begin{cases} i_1 = i_3 = \frac{1}{2}i_A + i_d \\ i_2 = i_4 = \frac{1}{2}i_A - i_d \\ i_5 = i_7 = \frac{1}{2}i_A + (1 - m^2 - m)i_d \\ i_6 = i_8 = \frac{1}{2}i_A - (1 - m^2 + m)i_d \\ i_{T1} = m(m+1)i_d \\ i_{T2} = m(m-1)i_d \\ i_D = 2(1 - m^2)i_d \end{cases} \quad (8)$$

The magneto-motive forces (MMFs) of iron cores 1 and 2 are defined as F_1 and F_2 , respectively. Then the following formulae can be obtained:

$$i_+ = \frac{F_1 + F_2}{2N}$$

$$i_- = \frac{F_1 - F_2}{2N}$$
(9)

where $2N$ is the number of turns. The expression of magnetic flux, Φ_1 , Φ_2 , of the iron cores can be simplified as follows:

$$\begin{cases} 2N \frac{d\Phi_1}{dt} = \left(1 + m \frac{\delta_1}{1 - \delta_1}\right) u_A - 2R \left(\frac{F_1}{2N} + |m| \frac{\delta_1}{1 - \delta_1} i_-\right) \\ 2N \frac{d\Phi_2}{dt} = \left(1 - m \frac{\delta_1}{1 - \delta_1}\right) u_A - 2R \left(\frac{F_2}{2N} - |m| \frac{\delta_1}{1 - \delta_1} i_-\right) \\ 2N \frac{d\Phi_1}{dt} = \left(1 + m \frac{\delta_2}{1 - \delta_2}\right) u_A - 2R \left(\frac{F_1}{2N} + |m| \frac{\delta_2}{1 - \delta_2} i_-\right) \\ 2N \frac{d\Phi_2}{dt} = \left(1 - m \frac{\delta_2}{1 - \delta_2}\right) u_A - 2R \left(\frac{F_2}{2N} - |m| \frac{\delta_2}{1 - \delta_2} i_-\right) \end{cases} \quad (10)$$

where $\delta_1 = N_1/N$, $\delta_2 = N_2/N$, R is the resistance of the windings around one limb of the reactors. The model of MCR with multi-taps can be simplified furtherly, and the simplified model is illustrated in Fig. 5. When the tapping ratio is switched, some parameters of the MCR are also changed, which is different from the traditional MCR.

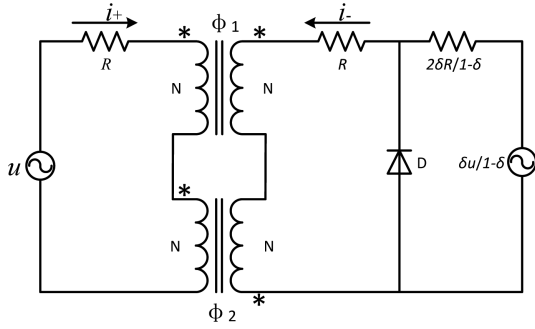


Fig. 5. Equivalent simulation model of MCR with multi-taps based on simplified mathematical model.

The firing angle α should be regulated. In addition, thyristors are used to realize full-wave rectification according to Fig. 5. This means that regulating α or switching taps can realize the regulation of DC biased voltage.

$$\begin{cases} u_c = m \frac{\delta}{1-\delta} u_A \\ = N \left(\frac{d\Phi_1}{dt} - \frac{d\Phi_2}{dt} \right) + \left(1 + m \frac{2\delta}{1-\delta} \right) Ri_- \\ i_c = i_- + |m| \frac{\delta}{1-\delta} i_- \\ u = N \left(\frac{d\Phi_1}{dt} + \frac{d\Phi_2}{dt} \right) + Ri_+ \\ i = i_+ + m \frac{\delta}{1-\delta} i_+ \end{cases} \quad (11)$$

where δ can be δ_1 or δ_2 . From the above analysis, the controlled DC component can be obtained according to Fig. 5 and (11).

$$I_0 = \frac{\delta U}{\pi(1+\delta)R} (1 + \cos \alpha) \quad (12)$$

To keep the controlled DC component constant, α should be regulated according to (12) when the tapping ratio is changed.

The DC controlled magnetic flux density B_d has linear correlation with the controlled direct current component. As mentioned in Fig. 4, the relationship between B_d and saturation degree β can be expressed:

$$\beta = 2 \cos^{-1} \frac{B_{sat} - B_d}{B_{sat}} \quad (13)$$

The amplitude value of the fundamental current of the MCR is given as

$$I_L = \frac{lB_{sat}}{2\pi N\mu_0} (\beta - \sin \beta) \quad (14)$$

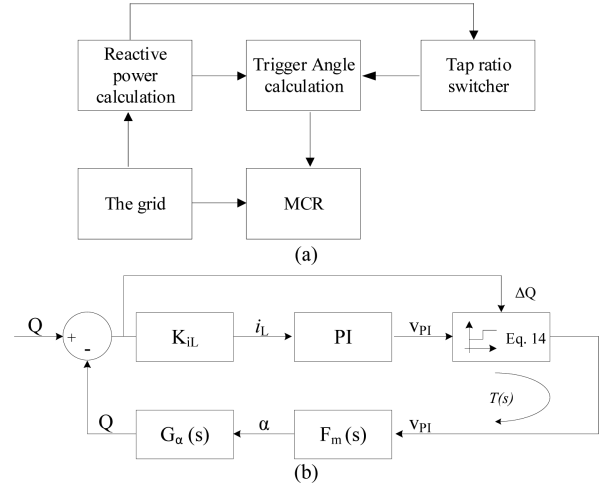


Fig. 6. Block diagram of MCR with multi-taps: (a) Overall structure, and (b) The structure of the algorithm.

where l is the height of the valves. Because the components of high frequency harmonics of MCR are very low, only the fundamental current is used to calculate the reactive power.

3. Proposed MCR with Multi-taps

A control algorithm is proposed to make multi-taps switching conveniently, as shown in Fig. 6.

The transfer function of PI controller is given as

$$\frac{\hat{V}_{PI}}{\hat{i}_L} = K_p \left(1 + \frac{1}{T_i s} \right) \quad (15)$$

where V_{PI} is the output of the PI controller, and i_L is the compensation current. The time delay resulted from the pulse width modulation (PWM) is half of a switching period. Thus, its small signal form is given as

$$F_m(s) = \frac{\pi}{V_p} e^{-\frac{T_s}{2}s} \quad (16)$$

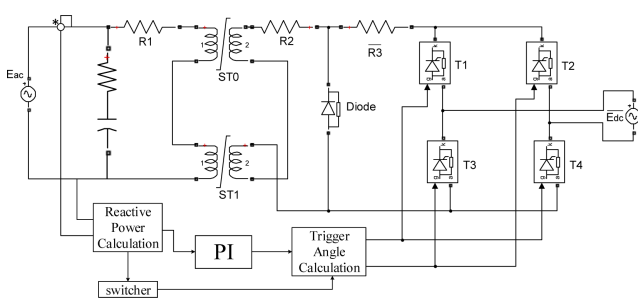
where V_p is the peak value of carrier, $T_s = 0.01$ s is the switching period and sampling period. According to [11], the transfer function of α corresponding to the reactive power Q can be obtained as

$$G_\alpha(s) = \frac{\hat{Q}}{\hat{\alpha}} \Big|_{i_c=0} = \frac{U_0 \hat{I}_L \sin \theta}{\hat{\theta}} \frac{\hat{\theta}}{\hat{B}_d} \frac{\hat{B}_d}{\hat{\alpha}} \quad (17)$$

where U_0 is the rated voltage of the grid, and θ is the power factor angle. Here, when the error of the reactive power from the grid is more than the threshold value, the tap switchers will be actuated, and α will change according to (14).

Table 1. Simulation Parameter Configuration in Simulink.

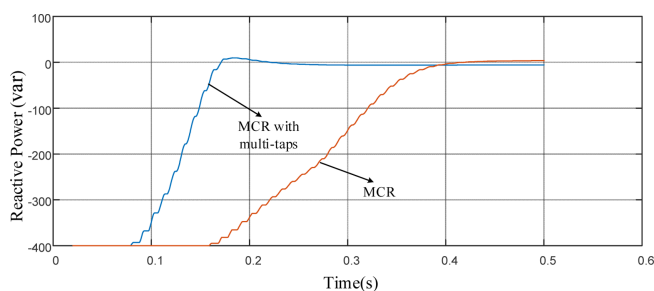
Component	Parameter	Value
Eac	Peak amplitude	537.32 V
Edc	Peak amplitude	28.28 V, 59.71 V
R1, R2	Resistance	5.15 Ω
R3	Resistance	0.54 Ω , 1.14 Ω
ST0, ST1	Rated reactive power	500 Var
δ	Tapping ratio	5 %, 10 %
Qc	Capacitive reactive power	400 Var
MCR	Saturation characteristic	[0 0; 0 1; 1 2]

**Fig. 7.** Simulation model of the MCR with multi-taps (500 VA/380 V).

4. Simulation Results and Analysis

A simulation model for MCR with multi-taps is shown in Fig. 7, which is based on the equivalent circuit as shown in Fig. 5. δ is set to 5 % and 10 %, respectively. The major simulation parameters are listed in Table 1, from which the saturation characteristics of the MCR is presented.

The capacitive reactive power of the grid is 400 Var, and the rated inductive reactive power of the MCR with multi-taps is 500 Var. Threshold value for the switch taps is 50 Var. The difference between the multi-taps MCR and traditional models is that there are two equivalent DC excitation sources, which present the different tapping ratios. According to (1), the MCR should be regulated

**Fig. 8.** (Color online) Reactive power regulated by MCR and MCR with multi-taps.

completely in 9.5 cycles (namely, 0.19 s) with $\delta = 10\%$ and in 4.5 cycles (namely, 0.09 s) with $\delta = 10\%$, respectively. From Fig. 8, the regulation time of the proposed MCR is about 0.1 s, and the traditional MCR is about 0.22 s. The simulations agree well with the theoretical calculations of regulated time, and the regulated time of this novel MCR is faster than that of the traditional one, which has been improved by over 50 %, as shown in Fig. 8. There is a temporary overshoot in the novel MCR system. Both of the taps share the same PI regulator parameters. Because the PI parameters should satisfy the stability of both taps, it is different from the single-tap MCR. In addition, the higher tap ratio may cause fewer stability margin, and the PI parameters tuning should be based on the higher tap ratio. Therefore, the lower tap ratio may be an underdamped system, and there is overshoot in the MCR with multi-taps system as shown in Fig. 8. The single tap ratio may be an overdamped system, and there is no overshoot in the traditional MCR system. Because the higher tapping ratio can provide higher DC voltage, the MCR with multi-taps can provide more increments of inductive reactive power than the traditional one during a sample period.

5. Conclusions

In this paper, a novel MCR with multi-taps is proposed to shorten the regulated time. The mathematical model of MCR with multi-taps is established and the operating principle of MCR with multi-taps is analyzed. According to the mathematical model of MCR, the algorithm of switching taps is written. The simulations agree well with the theoretical calculations of regulated time and this proves the reliability of the proposed algorithm.

Acknowledgment

This work was supported in part by the National Key R&D Program of China (2017YFB0903904), National Natural Science Foundation of China (No. 51777055, 51690181), and Hebei Province Science Foundation for Distinguished Young Scholars (No. E2018202284).

References

- [1] M. V. Biki and Yu. L. Chizhevskij, *Electrotehnika*, 9 (1994).
- [2] B. V. Oleksyuk, V. N. Tulsy, and S. Palis, *IEEE Trans. Power Delivery*, PP, 99.
- [3] S. Torseng, *IEE Proceedings C - Generation, Transmission and Distribution*, November **128**, 6 (1981).
- [4] G. Feng, J. Shao, S. Ma, and Y. Zhao, 2009 IEEE Inter-

- national Conference on Industrial Technology, Gippsland, VIC (2009) pp 1-4.
- [5] G. Feng, J. Shao, B. Zhang, and Y. Zhao, 2008 Joint International Conference on Power System Technology and IEEE Power India Conference, New Delhi (2008) pp 1-4.
- [6] T. Wass, S. Hornfeldt, and S. Valdemarsson, IEEE Trans. Magn. **42**, 9 (2006).
- [7] X. Chen, B. Chen, C. Tian, J. Yuan, and Y. Liu, IEEE Trans. Ind. Electron. **59**, 7 (2012).
- [8] X. Chen, J. Chen, and B. Chen, 2014 9th IEEE Conference on Industrial Electronics and Applications, Hangzhou, China (2014).
- [9] M. Tian, J. Li, P. Shi, and Y. Guo, IEEE Trans. Appl. Supercon **26**, 7 (2016).
- [10] Karymov, R. R. and M. Ebadian, Int. J. Elec. Power **29**, 3 (2007).
- [11] P. Wang, J. Zou, and X. Ma, IEEE Trans. Ind. Electron. **65**, 11 (2018).